

AFRL-SN-RS-TR-1999-28
Final Technical Report
February 1999



**DIGITAL AND ANALOG MODULATION OF FIBER
LASERS FOR HIGH-SPEED OPTICAL
COMMUNICATIONS AND CONTROL SYSTEMS**

KJT, Inc.

Kenneth J. Teegarden

APPROVED FOR PUBLIC RELEASE; DISTRIBUTION UNLIMITED.

19990323 054

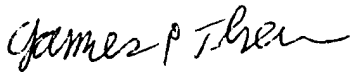
**AIR FORCE RESEARCH LABORATORY
SENSORS DIRECTORATE
ROME RESEARCH SITE
ROME, NEW YORK**

DTIC QUALITY INSPECTED 1

This report has been reviewed by the Air Force Research Laboratory, Information Directorate, Public Affairs Office (IFOIPA) and is releasable to the National Technical Information Service (NTIS). At NTIS it will be releasable to the general public, including foreign nations.

AFRL-SN-RS-TR-1999-28 has been reviewed and is approved for publication.

APPROVED:



JAMES P. THEIMER
Project Engineer

FOR THE DIRECTOR:



ROBERT G. POLCE, Acting Chief
Rome Operations Office
Sensors Directorate

If your address has changed or if you wish to be removed from the Air Force Research Laboratory Rome Research Site mailing list, or if the addressee is no longer employed by your organization, please notify AFRL/SNDR, 25 Electronic Parkway, Rome, NY 13441-4515. This will assist us in maintaining a current mailing list.

Do not return copies of this report unless contractual obligations or notices on a specific document require that it be returned.

REPORT DOCUMENTATION PAGE			Form Approved OMB No. 0704-0188	
<small>Public reporting burden for this collection of information is estimated to average 1 hour per response, including the time for reviewing instructions, searching existing data sources, gathering and maintaining the data needed, and completing and reviewing the collection of information. Send comments regarding this burden estimate or any other aspect of this collection of information, including suggestions for reducing this burden, to Washington Headquarters Services, Directorate for Information Operations and Reports, 1215 Jefferson Davis Highway, Suite 1204, Arlington, VA 22202-4302, and to the Office of Management and Budget, Paperwork Reduction Project (0704-0188), Washington, DC 20503.</small>				
1. AGENCY USE ONLY (Leave blank)	2. REPORT DATE February 1999	3. REPORT TYPE AND DATES COVERED Final Apr 97 - Apr 98		
4. TITLE AND SUBTITLE DIGITAL AND ANALOG MODULATION OF FIBER LASERS FOR HIGH-SPEED OPTICAL COMMUNICATIONS AND CONTROL SYSTEMS		5. FUNDING NUMBERS C - F30602-97-C-0126 PE - 62702F PR - 4600 TA - P6 WU - PA		
6. AUTHOR(S) Kenneth J. Teegarden				
7. PERFORMING ORGANIZATION NAME(S) AND ADDRESS(ES) KJT, Inc. 82 Westland Ave. Rochester NY 14618		8. PERFORMING ORGANIZATION REPORT NUMBER N/A		
9. SPONSORING/MONITORING AGENCY NAME(S) AND ADDRESS(ES) Air Force Research Laboratory/SNDR 25 Electronic Parkway Rome NY 13441-4515		10. SPONSORING/MONITORING AGENCY REPORT NUMBER AFRL-SN-RS-TR-1999-28		
11. SUPPLEMENTARY NOTES Air Force Research Laboratory Project Engineer: James P. Theimer/SNDR/(315) 330-4870				
12a. DISTRIBUTION AVAILABILITY STATEMENT Approved for public release; distribution unlimited.		12b. DISTRIBUTION CODE		
13. ABSTRACT (Maximum 200 words) This report describes the development of a mode-locked erbium-doped fiber laser. Active mode-locking was achieved by modulation of a multiple quantum well (MAW) device by Stark shifting the absorption of the quantum wells. The MQW device could also act as a saturable absorber, so that the laser could be passively mode-locked. Pulses as short as 11 pico seconds were produced. The cavity was injection mode-locked at both the fundamental and second harmonic period of the cavity round-trip time.				
14. SUBJECT TERMS Fiber Laser, Mode-Locking, Laser Noise, Injection Mode-Locking Multiple Quantum Well Devices			15. NUMBER OF PAGES 32	
			16. PRICE CODE	
17. SECURITY CLASSIFICATION OF REPORT UNCLASSIFIED	18. SECURITY CLASSIFICATION OF THIS PAGE UNCLASSIFIED	19. SECURITY CLASSIFICATION OF ABSTRACT UNCLASSIFIED	20. LIMITATION OF ABSTRACT UL	

Table of Contents

1.0 Introduction	PAGE 1
2.0 Optimization of the Passively Mode Locked Laser	1
2.1 EDFL Saturable Absorber Butt-Coupling Configuration	2
2.1.1 Optical Characterization of the MQW Saturable Absorbers	4
2.2 EDFL Saturable Absorber Free Space Coupling Configuration	9
2.3 Summary	11
3.0 Active Mode Locking of the Fiber Laser	12
3.1 Injection Mode Locking	12
3.1.1 Injection Locking at the Fundamental Frequency of the Linear Cavity	13
3.1.2 Injection Locking at the Second Harmonic	14
3.2 Summary	16
3.3 Electrical Mode Locking	16
4.0 References	19

List of Tables

Table 1. Summary of the pulse widths generated using the eight different saturable absorbers.	PAGE 4
Table 2. Summary of the measured carrier lifetime dynamics in the different saturable absorbers.	6

List of Figures

Fig. 1. Schematic diagram of the linear cavity erbium-doped fiber laser with the fiber butt-coupled to the MQW saturable absorber.	PAGE 2
Fig. 2. Enlarged schematic of the erbium-doped fiber-saturable absorber nonlinear mirror interface.	3
Fig. 3. a) Measured intensity autocorrelation and b) corresponding optical spectrum of the mode-locked pulses centered at 1555 nm using sample #1305.	5
Fig. 4. Linear absorbance spectrum of sample #1305.	5
Fig. 5. The experimental setup for the pump/probe measurements using a femtosecond Cr ⁴⁺ :YAG laser.	6
Fig. 6. Carrier recombination time in saturable absorber #1305.	7
Fig. 7. Comparison of the calculated and measured EDFL pulse widths as a function of the carrier lifetimes in the saturable absorbers.	8
Fig. 8. Schematic diagram of the linear cavity erbium-doped fiber laser with the light focused onto the MQW saturable absorber.	9
Fig. 9. a) Measured intensity autocorrelation and b) corresponding optical spectrum of the mode-locked pulses centered at 1556 nm using the chirped fiber Bragg grating as the laser output coupler and the gold substrate coated non-linear mirror structure.	11
Fig. 10. Set up for injection mode locking of the MQW laser.	12
Fig. 11. Synchronized output of the ring and linear cavity lasers.	13
Fig. 12. Optical spectrum and pulse duration of injected linear cavity laser.	14
Fig. 13. Output of MQW laser injection mode locked at its second harmonic.	15
Fig. 14. Power spectrum of the MQW laser operating at its second harmonic.	16
Fig. 15. Quantum well absorption spectra as a function of applied voltage.	18
Fig. 16. Calculated reflectivity, R, of the saturable absorber as a function of applied voltage.	18
Fig. 17. Reflectivity of a saturable absorber in a Fabry Perot etalon.	19

1.0 Introduction

Earlier work has resulted in the design and construction of a new passively mode locked fiber laser prototype. By combining fiber grating technology with a unique quantum well saturable absorber (QW absorber), an erbium doped fiber laser operating with unusually low pump power and producing mode locked pulses of 10 ps duration and a repetition rate of 3.5 MHz was constructed. Although compact and insensitive to vibration, this design, which was based on butt coupling one end of the laser cavity to the QW absorber, produced short output pulses superimposed on a pedestal or quasi DC component. Also, it was found difficult to reproducibly manufacture quantum well absorbers which produced 10 ps pulse duration with low threshold for mode locking. The objective of much of the work described in this report was to reduce pulse duration and improve pulse shape in this passively mode locked laser by optimizing the design of the QW absorber and fiber grating, and improving the coupling of the cavity to the QW absorber. In order to better understand the role of the saturable absorber in determining pulse shape and duration, and optimize its performance, measurements of non linear absorption and the temporal behavior of its absorption were initiated. Also, a new method of coupling to the QW absorber was developed and a chirped fiber grating designed to increase the available gain band width was used instead of the linear grating employed earlier.

Another problem with the passively mode locked laser is that the fundamental frequency of the mode locked pulses is too low for several important applications. The frequency could be increased by shortening the cavity length by perhaps a factor of 10, but a frequency above 100 MHz is probably not obtainable by this means. Also, the synchronization of short pulse fiber lasers is a requirement for their use in high speed optical communications systems where optical clock recovery is important. Active mode locking would provide a way of operating the laser at a high harmonic of the fundamental frequency. Two ways of actively mode locking the fiber laser were explored as part of this project.

2.0 Optimization of the Passively Mode Locked Laser

Compact sources of ultrashort optical pulses in the 1.55 μm region have been the subject of much research in recent years. Turn-key and efficient operation must first be achieved if these lasers are to be practically implemented in applications such as high-speed optical networks, fiber-based interconnects and photonic analog to digital (A/D) converters. One source which has received considerable attention is the erbium-doped fiber laser (EDFL).[1] In addition to being compatible with standard telecommunication grade optical fiber, mode-locked EDFLs can provide high repetition rates, high intensities, large spectral bandwidths and high timing stability. Passively mode-locked EDFLs have been demonstrated in a variety of cavity configurations. The figure-eight laser uses additive pulse mode-locking (APM) which converts non-linear self-phase modulation (SPM) into ultrafast amplitude modulation.[2] Nonlinear polarization evolution used in conjunction with a polarizer in

a ring cavity configuration is another proven technique which provides the ultrafast modulation required for passive mode-locking.[3]

The use of multiple quantum well (MQW) semiconductor saturable absorbers (SAs) placed within the EDFL cavity provide an alternative to APM techniques. The semiconductor saturable absorbers have been shown to be an effective method for creating self-starting mode-locked fiber lasers.[4,5] Unlike APM fiber lasers which require ultra-sensitive control of the cavity birefringence to maintain optimum operation, these lasers are immune to changes in the cavity birefringence. Saturable absorbers also have low saturation intensities which makes them compatible with low gain erbium-doped fiber and commercially available diode pumping schemes. These extremely important qualities make them a practical choice for turn-key remote operation. This paper will discuss the operation of a linear cavity EDFL mode-locked laser with a variety of semiconductor saturable absorbers. The effects of the optical properties of the saturable absorbers will be examined as well as the effects of different cavity configurations upon mode-locked operation.

2.1 EDFL Saturable Absorber Butt-Coupling Configuration

The setup of the EDFL initially used in this work is shown in Fig. 1. The gain medium originally consisted of 22.5 m of erbium-doped fiber that was directly butt-coupled to the MQW saturable absorber that served as the high reflector at the back end of the cavity. The other end of the erbium-doped fiber was fusion spliced to a fiber Bragg grating which served as the output coupler of the laser. The 49% peak reflectance of this grating is centered at 1556 nm with a FWHM spectral bandwidth of 1.0 nm. The laser was pumped with approximately 80 mW at 980 nm with a laser diode (BFSWA0980SDL1180AB) obtained from SDL Optics. The output of the laser was taken through the other available port of the WDM.

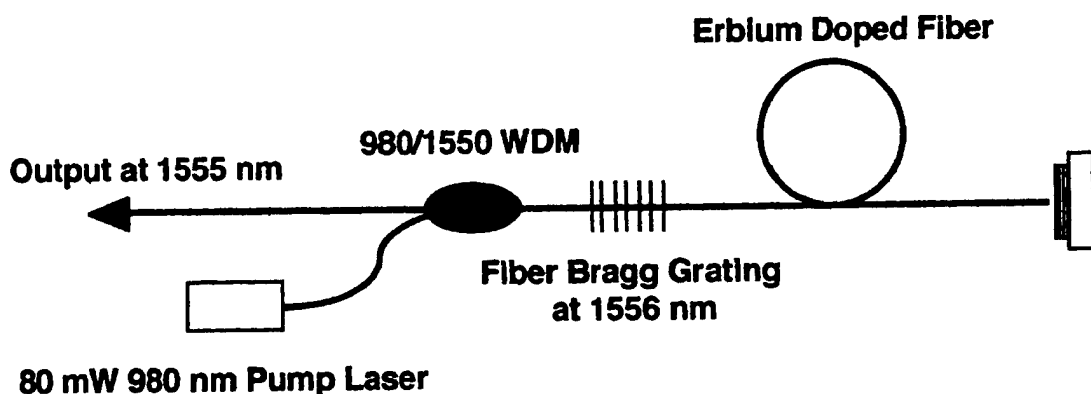


Fig. 1. Schematic diagram of the linear cavity erbium-doped fiber laser with the fiber butt-coupled to the MQW saturable absorber.

The MQW saturable absorbers were used as both the mode-locking element and the back mirror of the laser cavity. The SAs consisted of 50 periods of MQW layers grown

on top of a semi-insulating InP substrate. The quantum well region in seven of the samples used in this portion of the work consisted of 100 Å $\text{In}_{0.53}\text{Ga}_{0.47}\text{As}$ wells and 100 Å $\text{In}_{0.52}\text{Al}_{0.48}\text{As}$ barriers. The sample denoted as #1442 consisted of 100 Å $\text{In}_{0.53}\text{Ga}_{0.47}\text{As}$ wells and 100 Å InP barriers. The differences in these samples is the result of different growth temperatures and also post-processing such as ion implantation. The resulting carrier lifetime differences among the eight samples will be examined later in this section.

The mirror action of the SA arose from Fresnel reflections at the front and back surfaces of the device. None of the devices used in the initial work contained a high reflector at the back of MQW region. The erbium-doped fiber was typically separated from the SA by approximately 10 μm . Fig. 2 shows an enlarged view of the fiber - saturable absorber non-linear mirror interface. The coupling of light back into the fiber was calculated to be less than 1.5%. The reduced reflection results in lower coupling back into the absorber and slightly larger pulse widths. Fortunately the high gain of the erbium-fiber was able compensate for this very large cavity loss.

The eight saturable absorbers were examined as the mode-locking element within the EDFL cavity. Only the SAs were changed at the back end of the laser cavity. The rest of the configuration remained the same. The laser was characterized for each SA to determine the minimum, maximum, and average pulse width. The results are summarized in Table 1. The values were recorded as the lateral position of the fiber along the SA was varied. There was much variation as the incident spot on the SA was moved. Changes in the pulse width or movement from pure cw mode-locking to the q-switched mode-locking regime were observed for movements as little as 10 μm . This is attributable at least in part to changes in the carrier lifetime as the position is changed on the saturable absorber. It is also caused by changes in the reflection of the saturable absorber to due growth inhomogeneities.

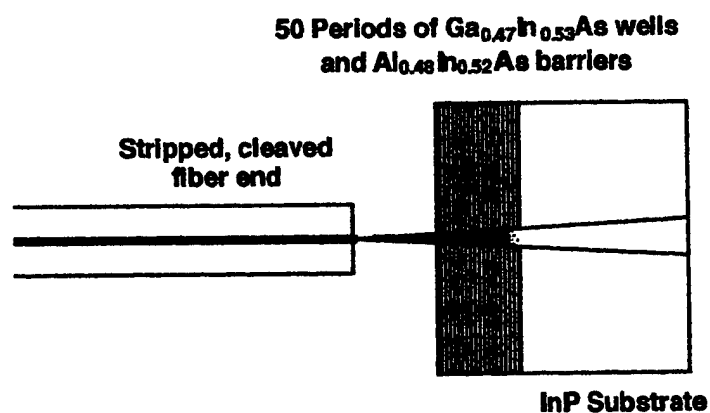


Fig. 2. Enlarged schematic of the erbium-doped fiber - saturable absorber nonlinear mirror interface.

Sample	τ_{min} (ps)	τ_{max} (ps)	τ_{ave} (ps)
1305	11.1	19.3	14.2
1442	20.1	49.7	35.2
1590	28.6	52.7	38.8
1590 ii.	17.9	39.3	29.3
1629	26.2	45.5	34.3
1641	29.9	46.2	36.9
1643	20.8	30.0	25.5
1650	18.5	29.6	23.9

Table 1. Summary of the pulse widths generated using the eight different saturable absorbers.

A typical autocorrelation and mode-locked optical spectrum centered at 1555 nm is shown in Fig. 3. The traces were recorded using sample #1305 and correspond to an average output power of 2.2 mW. The repetition rate in the cavity was approximately 4.4 MHz. Assuming a hyperbolic secant squared pulse shape, the time bandwidth product is 0.46 which deviates from the transform limited value of 0.32. The average output power for all of the SAs tested ranged from 6.7 to 0.2 mW.

The autocorrelation trace shown in Fig 3a illustrates one of the problems encountered with the butt coupled configuration. The short mode locked pulses were superimposed on a broad pedestal. A large fraction of the output power of the laser was contained in this pedestal, greatly reducing the peak power of the pulses. In addition, measurements of the relative intensity noise (RIN) were made and a value as high as 20% was observed. For this reason no attempt was made to measure bit error rate using this laser. Instead, efforts were directed towards reducing the the pedestal and the RIN by improving the performance of the saturable absorber and its coupling to the cavity.

2.1.1 Optical Characterization of the MQW Saturable Absorbers

This section explores some of the optical properties of the SAs that contribute to pulse formation within the EDFL. The linear absorbance spectrum of sample #1305 is shown in Fig. 4. The quantum well widths were 100 Å in all of the samples which correspond to the heavy hole excitonic band-edge being at approximately 1575 nm. The placement of the band-edge at the longer wavelengths ensured adequate depth of modulation at 1555 nm within the high gain EDFL cavity.

A degenerate, co-linear, pump/probe experimental setup as shown in Fig. 5 was used to measure the carrier lifetimes of the MQWs. A tunable femtosecond Cr⁺⁺:YAG laser mode-locked by a unique saturable absorber mirror structure was used as the pulsed source in the experiment.[6] The laser produces a minimum of 120 fs pulses at 1488 nm and is tunable from 1488 to 1535 nm. The laser was run at its free running wavelength of 1507 nm during the pump/probe experiments. The pump and probe beams were separated into orthogonal polarizations by a 50/50 polarizing beam splitter. The probe beam was delayed with respect to the pump beam using a linear

stage controlled with a stepper motor. The stage provided up to 10 cm of travel. The beams were then recombined co-linearly using a nonpolarizing beam splitter and focused onto the sample using a 10X microscope objective. The transmitted light was re-collimated with a 10X microscope objective. The spot size on the sample was

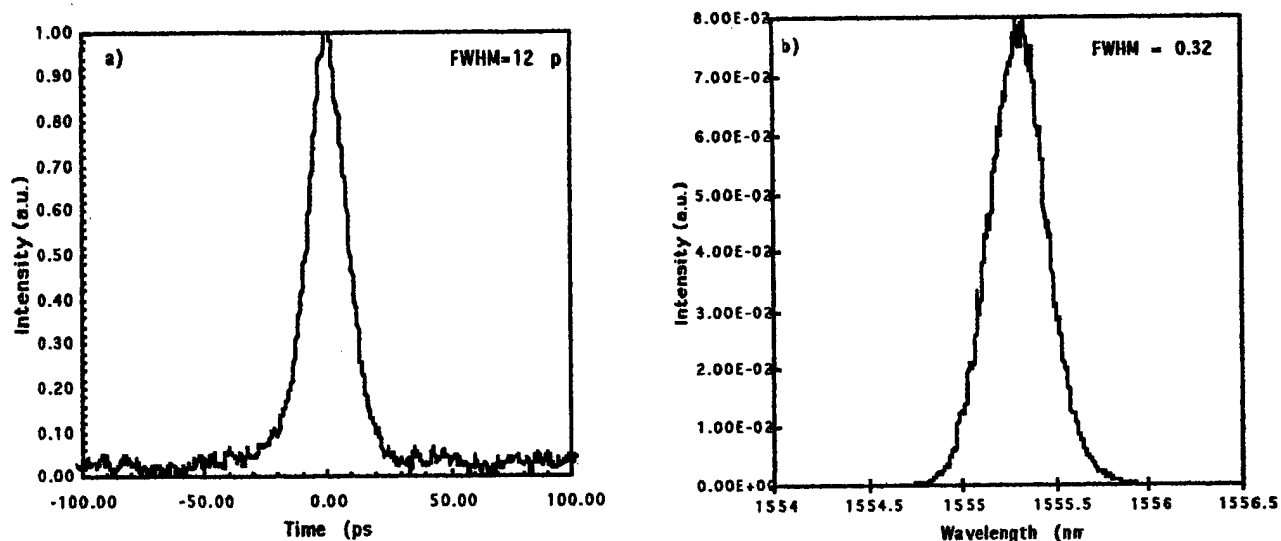


Fig. 3. a) Measured Intensity autocorrelation and b) corresponding optical spectrum of the mode-locked pulses centered at 1555 nm using sample #1305.

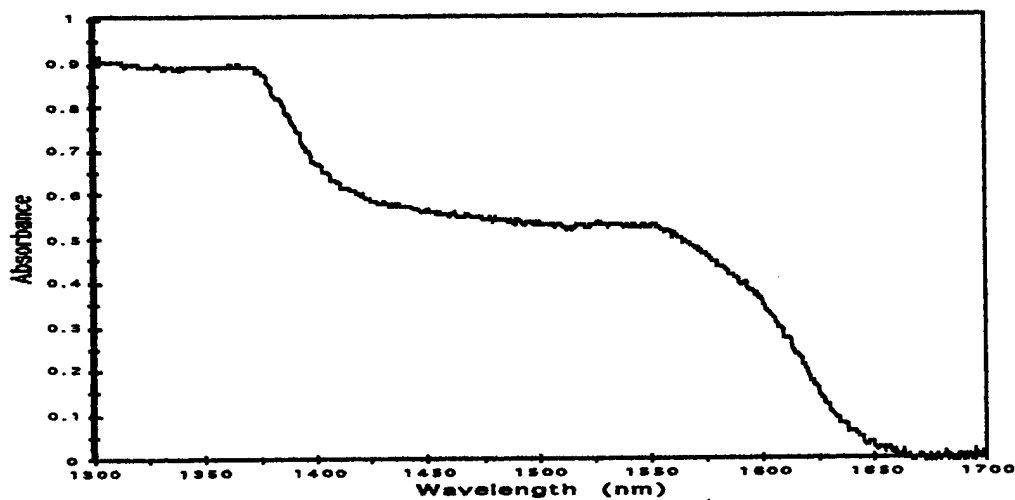


Fig. 4. Linear absorbance spectrum of sample #1305.

calculated to be approximately 16 μm . A Glan-Thompson polarizer was then used to reject the pump beam ensuring that only the transmitted probe beam reached the detector. The probe beam was focused onto a Ge detector using a 5 cm focal length lens. The detector was connected to a transimpedance amplifier and then to a lock-in

amplifier. The data was then collected by a computer which also controlled the movement of the linear stage. An optical chopper provided the reference signal to the

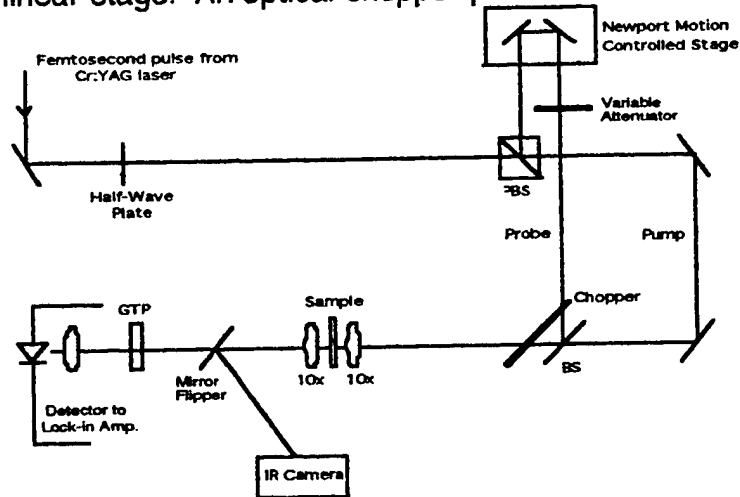


Fig.5. The experimental setup for the pump/probe measurements using a femtosecond Cr⁴⁺:YAG laser.

lock-in amplifier and cut both the pump and probe beams but at different frequencies. This allowed a differential lock-in technique to be used so that only the pump induced change in the probe transmission was detected. The pump to probe ratio was set at either 50:1 or 100:1 depending upon the sample used. The average pump power present at the sample was approximately 8 mW.

Table 2 summarizes the results of the pump/probe experiments for all eight of the MQW saturable absorbers. The average lifetime of each sample is recorded along with its minimum and maximum values. The lifetime of the carriers was once again found to be a function of position on the saturable absorber. A minimum of five different positions on each saturable absorber was examined. Fig. 6 shows the differential transmission for sample #1305 which is fit to an exponential recovery time constant of 264 ps. Sample #1590 and #1442 were found to have very long lifetimes on the order of 2 ns which were much longer than the 400 ps time scale of the experiment. It was therefore very difficult to differentiate between the time constants of the multiple scans. It should also be noted that the samples with the lowest MBE growth temperatures such as #1629 and #1650 exhibited the fastest recovery times as was expected.

Sample	τ_{min} (ps)	τ_{max} (ps)	τ_{avg} (ps)
1305	239	325	271
1442	2000	2000	2000
1590	2000	2000	2000
1590 ii.	199	352	277
1629	37	44	40
1641	611	1200	799
1643	455	634	533
1650	102	113	109

Table 2. Summary of the measured carrier lifetime dynamics in the different saturable absorbers.

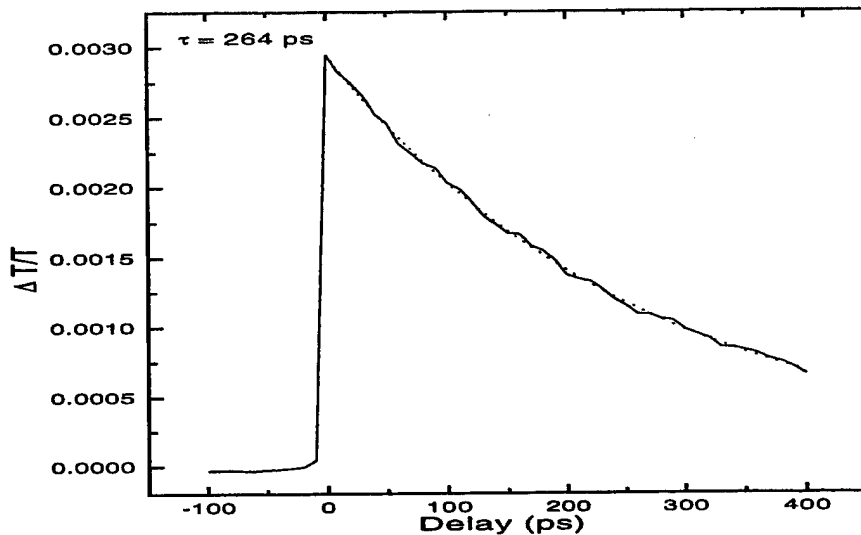


Fig 6. Carrier recombination time in saturable absorber #1305. The dashed curve is an exponential fit to the measured data indicating a recovery time of 264 ps.

The relationship between the carrier lifetimes of the SAs and the pulse widths produced by the EDFL cannot be explained by either fast saturable absorber (FSA) mode-locking or slow saturable absorber (SSA) mode-locking with gain saturation.[7,8] The carrier lifetimes are much longer in all instances than the pulse widths. The two would have to be on the same order for FSA mode-locking. SSA mode-locking with gain saturation does not occur in EDFLs because of the very long upper state lifetimes which makes them hard to saturate. The laser is best described by soliton mode-locking theory even though the laser in this configuration does not support true solitons due to the large losses suffered at the butt-coupled back mirror and at the fiber grating output coupler. It has been demonstrated that soliton mode-locking with a slow saturable absorber results in pulse widths much shorter than the carrier lifetime of the saturable absorber.[9,10]

The minimum obtainable pulse width, τ_p that can be generated from a laser using soliton pulse shaping with a saturable absorber was calculated using

$$\tau_p = \left(\frac{1}{\sqrt{6}\Omega} \right)^{\frac{3}{4}} \left(\frac{T_a g^{\frac{3}{2}}}{q_0} \right)^{\frac{1}{4}} (\phi)^{\frac{1}{8}} \quad (1)$$

where Ω is the gain bandwidth of the laser, T_a is the saturable absorber lifetime, g is the saturated laser gain, q_0 is the unsaturated loss of the saturable absorber, and ϕ is the nonlinear phase shift per round trip due to SPM.[10] The gain bandwidth of the erbium is limited by the 1 nm linewidth of the fiber grating output coupler and the very narrow Fabry-Perot reflectance spectrum of the saturable absorber structure. The

shows the experimental and calculated pulse widths obtained from the fiber laser as a function of the lifetime of the saturable absorber.

It should be noted that sample #1629 which had a measured recovery time of 40 ps was excluded from this fit. This saturable absorber generated multiple pulses per cavity round trip. The multiple pulses were noisy and distributed randomly in time. As the laser tries to form very narrow pulses using this saturable absorber, the corresponding pulse energy increases past a certain stability limit. The laser will now prefer to see extra pulses per cavity round trip each having a much lower energy than the single high energy pulse.[11,12] The pulse widths will now be longer than expected because the decreased pulse energy of the multiple pulses creates less self-phase modulation and directly results in longer pulse durations. Sample #1629 had an average measured pulse width of 34.3 ps which was much larger than the calculated value of 16.5 ps. The pump power of the EDFL was reduced from 80 to 32 mW which was just above lasing threshold in hopes of eliminating the multiple pulses. The multi-pulsing was greatly reduced at this pump level but flashes of extra pulses were occasionally present and the pulses remained very long. Finally, the pump power was set at approximately 40 mW and part of the erbium fiber was intentionally twisted to introduce extra loss into the cavity. This appeared to eliminate all of the extra pulses and a pulse width of 30 ps was measured. However, the optimum pulse width was still not achieved because the low pump powers limited the depth of modulation of the saturable absorber.

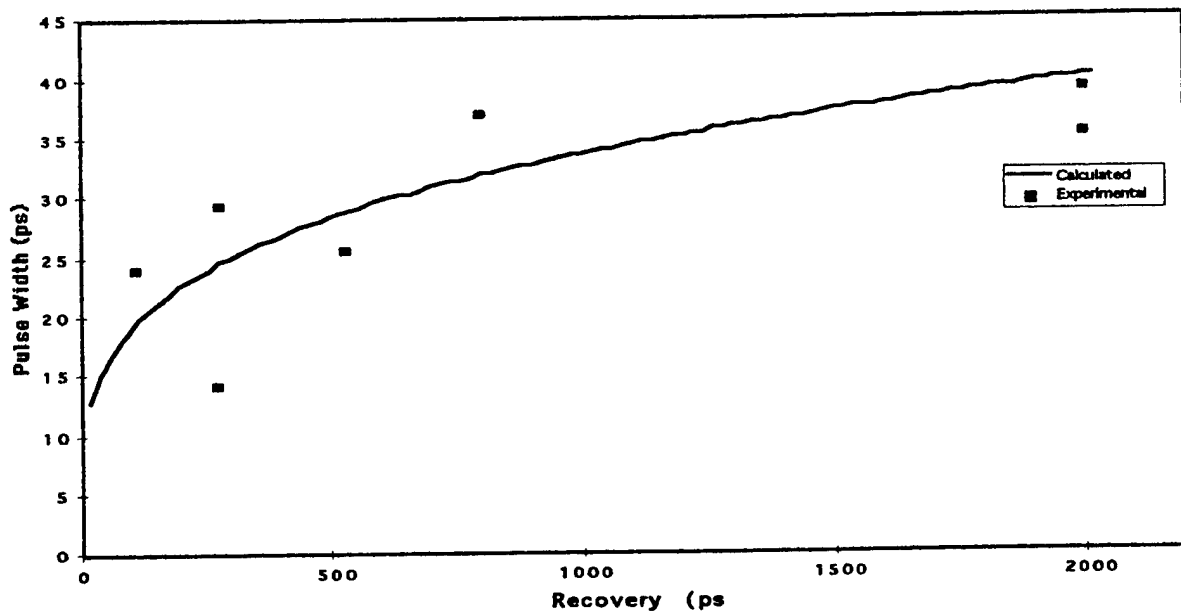


Fig. 7. Comparison of the calculated and measured EDFL pulse widths as a function of the carrier lifetimes in the saturable absorbers.

2.2 EDFL Saturable Absorber Free Space Coupling Configuration

The butt-coupling of the erbium-doped fiber to the MQW saturable absorber forms a very compact laser cavity. The EDFL contains all fiber components which are easily spliced together. No free space elements are required. However, the large losses in the cavity which are mainly due to the poor back mirror coupling limited true soliton pulse shaping. The pulses also contained a large pedestal and suffered from large amplitude fluctuations. The laser cavity was slightly modified in hopes of producing quieter, background free pulses. The modified laser cavity is shown in Fig. 8. The direct butt-coupling of the fiber to the absorber was replaced with a free space section consisting of two microscope objectives which acted as both collimating and focusing lenses. This setup had an optimal coupling efficiency of approximately 30%. This is a drastic improvement over the 1% coupling achieved with the butt-coupling setup. The erbium-doped fiber used in the original setup was replaced with highly doped fiber obtained from the Naval Research Laboratory. The fiber was characterized as having 1.0 dB/mW of absorption and a dispersion of 11 ± 3 ps/nm·km. A short length of standard SMF-28 was spliced to the 2.5 m of the erbium-fiber which increased the cavity length to 6.7 m, corresponding to a fundamental repetition rate of 14.9 MHz.

The temporal and spectral pulse widths produced by the EDFL in this modified configuration were very similar to those produced in the butt-coupled configuration. However, the pulses did not contain the large pedestals and the RIN was reduced to less than 1.0%. The temporal noise properties of the EDFL were also analyzed using this modified cavity. The power spectrum of the pulse train was analyzed using the theory proposed by von der Linde to provide a measure of the timing jitter.[13] The laser exhibited timing jitter less than 1 ps which is extremely small for a passively mode-locked fiber laser. The narrow spectral bandwidth of the fiber Bragg grating output coupler in conjunction with the narrow reflection band and high loss of the MQW saturable absorber are the apparent causes of this low timing jitter.[14]

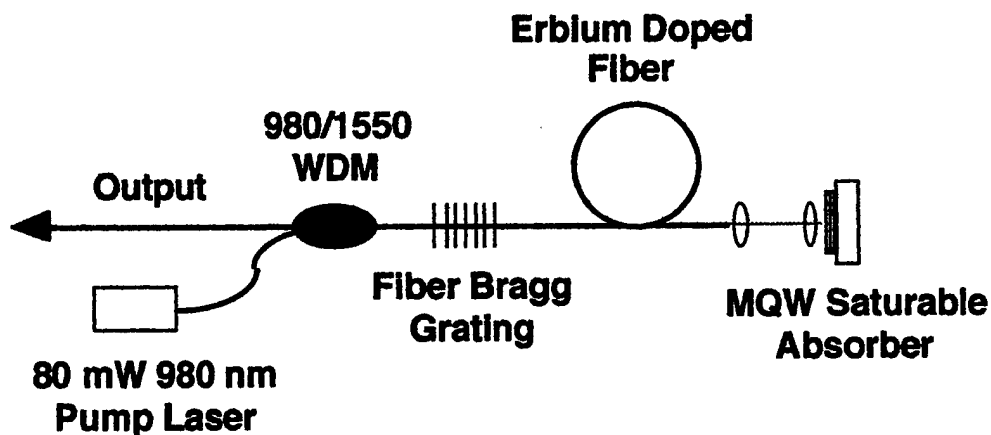


Fig. 8. Schematic diagram of the linear cavity erbium-doped fiber laser with the light focused onto the MQW saturable absorber.

In order to further reduce the overall loss of the EDFL cavity, an effort was made to reduce the loss of the non-linear saturable absorber mirror structure through the use of a highly reflective back coating. The lack of certain epitaxial growth resources limited the available options for the high reflector. Growth of an integrated quarter wave stack was not possible. Another option was pursued which first involved thinning the InP substrate to approximately 50 μm . The remaining substrate was then coated with gold, thus providing a very highly reflective back surface. The decrease in cavity loss allowed further shortening of the temporal pulse widths. For example a 50 period sample that was thinned and gold coated, resulted in a decrease in pulse width from 20.0 to 8.9 ps. The decreased pulse width is also attributable to the increased reflection resonance linewidth resulting from the thinned substrate.

The dispersive properties of the EDFL were also examined. The fiber Bragg grating at the output coupler was replaced with a chirped Bragg grating. These specialty fiber gratings provide very large amounts of chromatic dispersion over a very short distance. In essence a single chirped grating can replace the dispersion provided by many kilometers of standard fiber. The sign of the dispersion that is provided by the grating is dependent upon its orientation. The chirped grating was examined in the EDFL cavity in both possible dispersion orientations. In the first direction which corresponded to net normal dispersion, the pulse widths were slightly shorter than with the regular grating but the spectrums were very asymmetric and unstable. Upon reversing the grating and providing net negative dispersion, much shorter pulses were formed with very symmetric spectrums. Sidebands were also observed on the spectrums for the first time indicating the presence of soliton pulse shaping. Fig. 9 shows a typical autocorrelation and mode-locked spectrum for the EDFL which contained the chirped Bragg grating and the gold coated SA structure. The pulse width is 3.1 ps with a corresponding optical spectrum of 1.12 nm. The time bandwidth product is 0.43 which is slightly above the transform limited value of 0.32 for a hyperbolic secant squared pulse shape.

Finally a 90/10 optical splitter was inserted within the EDFL cavity immediately before the saturable absorber. This allowed us to tap off a small portion of the cavity's energy so that the pulse before and after interaction with the SA could be observed. The dispersive effects of both the quantum wells and the erbium fiber in conjunction with the chirped grating can be investigated using this method. The temporal and spectral pulse shapes were very similar before and after interaction with the SA. Only after further external cavity propagation through long lengths of standard single-mode fiber was there a discernible change in pulse shape. The pulse that is tapped from the cavity immediately before the SA retains its temporal width and shape after propagation through long lengths of fiber. However, the pulse tapped from the cavity immediately after the SA begins to widen in time as it travels through fiber. After only 4 km it has widened to approximately 30 ps. This indicates that the pulse is effectively chirped by the SA and that the added dispersion of the optical fiber drastically alters the pulse shape. It also appears that the dispersion compensation provided by the chirped Bragg grating effectively compensates for the dispersion of the SA. Further

experiments will be performed in the near future to quantify the actual dispersive values of the different intracavity elements.

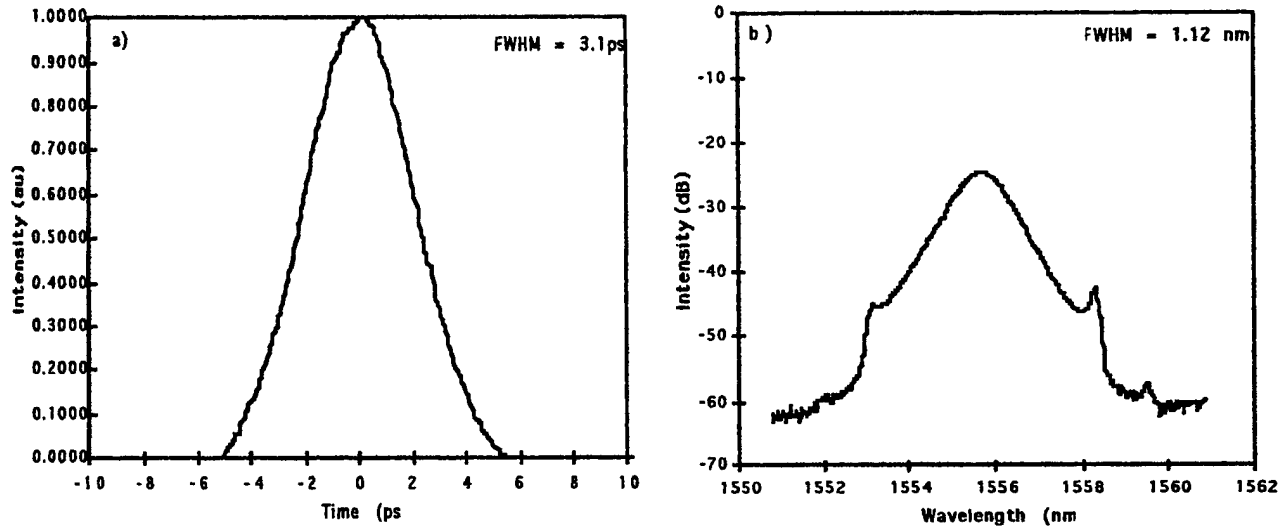


Fig. 9. a) Measured intensity autocorrelation and b) corresponding optical spectrum of the mode-locked pulses centered at 1556 nm using the chirped fiber Bragg grating as the laser output coupler and the gold substrate coated non-linear mirror structure.

2.3 Summary

We have demonstrated the operation of a linear cavity EDFL mode-locked with a variety of 50 period MQW saturable absorbers using different cavity configurations. A compact cavity which simply butt-coupled the erbium-doped fiber to the MQW saturable absorber was first examined. Pulse widths ranging from 14.2 to 38.8 ps were generated using a series of saturable absorbers whose optical properties had been modified. It was found in this cavity configuration that the lifetimes of the carriers in the MQWs were the primary optical property that determined the final pulse widths. A second cavity configuration was also examined which used microscope objectives to collimate and focus the light onto the saturable absorber. This improved cavity layout eliminated the amplitude fluctuations in the pulse train and also removed the background pedestal. Improvements to the saturable absorber mirror structure were also made to reduce the overall loss within the cavity. The InP substrate was thinned and gold coated which reduced its loss and greatly improved the overall coupling efficiency back into the optical fiber. This resulted in reduced pulse widths. A chirped fiber Bragg grating was also inserted as the output coupler of the EDFL. Soliton pulse shaping was observed and pulse widths on the order of 3 ps were generated. Further experiments will be performed to quantify this dispersion in order to subsequently manage the dispersion of the entire cavity thereby allowing the production of transform-limited soliton pulses.

3.0 Active Mode Locking of the Fiber Laser

As mentioned above, the long cavity lengths generally found in fiber lasers result in pulse periods which limit application to high speed optical communications systems. One way of increasing the repetition rate of the passively mode locked laser is to injection mode lock it at high multiples of the fundamental cavity frequency.

3.1 Injection Mode Locking

Injection mode locking of a passively mode locked laser requires the generation of a pulse stream to act as a master signal. In our case the master signal was produced by an actively mode locked fiber ring laser. The general experimental layout is shown in Fig. 10. A 3dB coupler was used to inject the pulse train from the ring laser into the WDM of the linear cavity passively mode locked laser shown in Fig. 1. To compensate for the loss of power in this coupler an erbium fiber amplifier was constructed to boost the power from the ring laser. This amplifier consisted of 15 m of ATT EDF-HE980 erbium doped fiber pumped by approximately 90 mW at 980 nm. The ring laser developed an average power of 1.35 mW which was amplified by 11.8 dB to 20.6 mW. The amplifier boosted the peak power of the mode locked pulses from the ring laser to a level high enough to modulate the saturable absorber in the passively mode locked laser. The mode locked train from the ring laser entered the linear cavity through a fiber Bragg grating. Provided there is no spectral overlap between the injected pulses and the reflection band of the grating, the pulses enter the linear cavity with little attenuation. Adjustments to the polarization controller in the ring laser were used to obtain this condition.

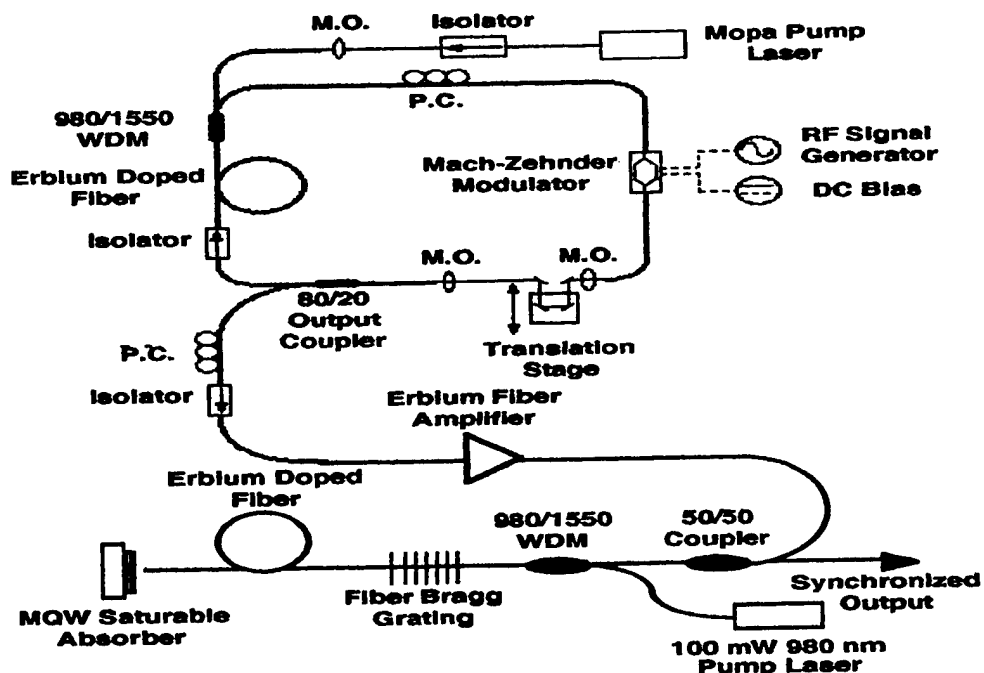


Fig. 10. Set up for Injection mode locking of MQW laser

The output of the MQW laser was incident on a fast photodetector and observed on an oscilloscope. The oscilloscope was triggered by the signal generator modulating the ring laser. Only when the two lasers were temporally synchronized could the MQW laser output be observed stably on the oscilloscope. In some cases the observed pulses would simply be the amplified re-emission of the injected signal. Passing through the MQW laser cavity, the injected signal could reduce the gain available to the MQW laser. In this case there would be no observable output from the linear cavity. Only when the MQW laser spectrum was present and exhibited broadening along with a stable train could the lasers be said to be synchronized.

3.1.1 Injection Locking at the Fundamental Frequency of the Linear Cavity

The MQW laser operated at a fundamental repetition rate of 3.5435 MHz and the cavity of the ring laser was adjusted to match this frequency within 100 Hz. The ring laser peak wavelength was adjusted to 1558 nm using the polarization controller. Its mode locked pulse duration was 3.0 ps with a spectral width of 1.5 nm. The lasers began synchronized operation at a threshold injected power of approximately 1.5 mW, corresponding to a peak power of 140 W and a pulse energy of 400 pJ. The synchronized output of the two lasers is shown in Fig 11.

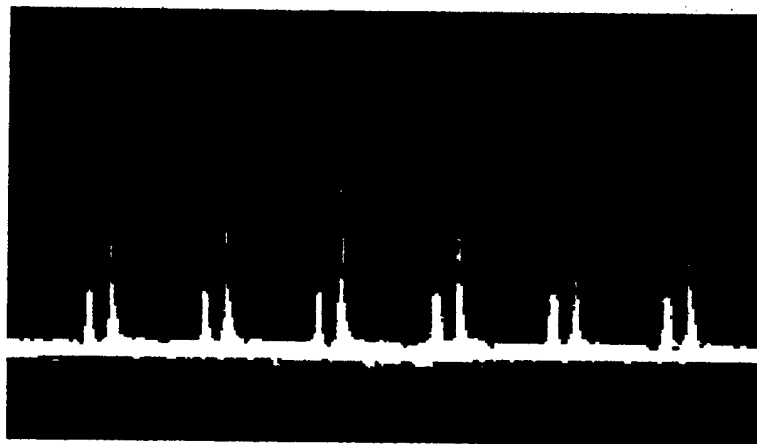


Fig. 11. Synchronized output of the ring and linear cavity lasers

The pulse duration of the MQW laser varied from 9.0 to 30 ps, similar to the durations produced when the laser was running freely. Also, the pulse width depended critically on the position of the fiber on the MQW mirror rather than on the power of the ring laser. This seems to indicate that the injected signal serves only to control the timing of the MQW laser cavity and there is no additional modulation due to the injected signal within the resonator. The MQW laser output contained both the ring laser and linear cavity laser spectra. the latter is shown in Fig 12.

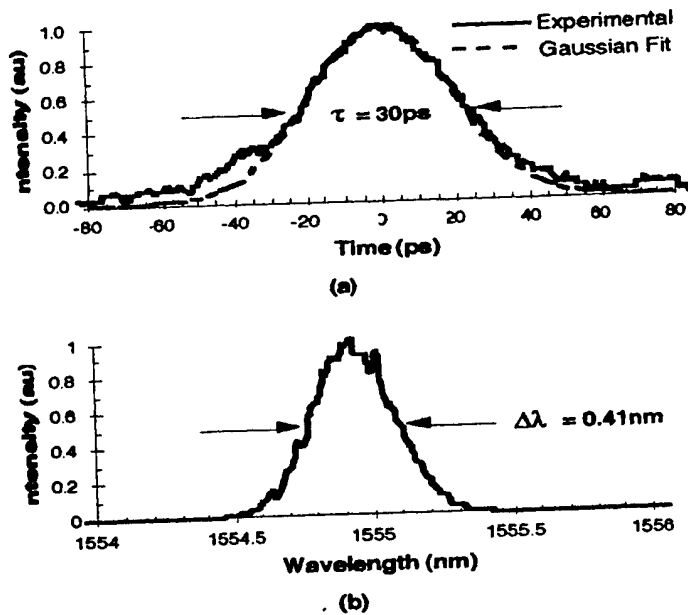


Fig. 12. Output spectrum and pulse duration of injected linear cavity laser

The output from the ring laser was more than 10 dBm below that of the MQW laser ensuring that the observed output is indeed that of the injection mode locked MQW laser and not amplified readmission of the ring laser signal.

The ring cavity was detuned from the operating frequency of 3.5435 MHz to determine the range of frequencies over which injection mode locking would occur. The lasers demonstrated synchronization over a frequency range from 3.54358 MHz to 3.54320 MHz providing an effective fractional bandwidth of 1.83×10^{-4} . As the detuning increased it became necessary to inject pulses of a higher peak power to maintain synchronization. The greatest detuning limits required injection powers in excess of 5.0 mW.

3.1.2 Injection Locking at the Second Harmonic

The butt-coupled configuration of the linear cavity laser shown in Fig. 1 proved unable to support injection mode locking at harmonics of the laser cavity. The system was therefore redesigned to include the free space optics shown in Fig 8. This reduced losses within the linear cavity as described above. The cavity length was reduced to permit operation at a fundamental repetition rate of 20 MHz. The ring cavity was also redesigned to operate at approximately 5.0 MHz. Although this required operation at the fourth harmonic of the cavity and thus reduced the available energy per pulse by a factor of 4, the additional span of fiber was required to obtain sufficient nonlinear polarization rotation to maintain short, stable output pulses. Approximately 9.0 mW of power was injected into the linear cavity laser. With a 3.0 ps pulse the peak power was approximately 150 W corresponding to a pulse energy of energy of 450 pJ.

At this injected power level, the MQW laser was induced to operate at the second harmonic of its fundamental repetition rate. However, the injected signal was insufficient to completely lock the MQW laser output to the ring laser output. The output of the MQW laser running at its second harmonic is shown in Fig. 13. It exhibited the spectral broadening characteristic of the linear cavity laser. An examination of the power spectrum of the MQW laser showed a reduction of power at the fundamental cavity frequency of more than 20 dBm relative to delta function peak observed in the power spectrum at the operating repetition rate of approximately 40 MHz. This reduction, shown in Fig. 14, confirmed that the laser was indeed operating at its second harmonic.

Attempts to operate the MQW laser at higher harmonics failed because the injected powers were insufficient to perturb the saturable absorber. The high loss in the cavity due to the low reflectivity of the saturable absorber reduced the energy available to support multiple pulses in the cavity. Reduction of this loss by the incorporation of a distributed Bragg reflector beneath the MQW stack would greatly increase the available energy in the cavity. The ultimate limit on the repetition rate is the recovery time of the saturable absorber which in this case was 270 ps. or a rate of about 4 GHz.

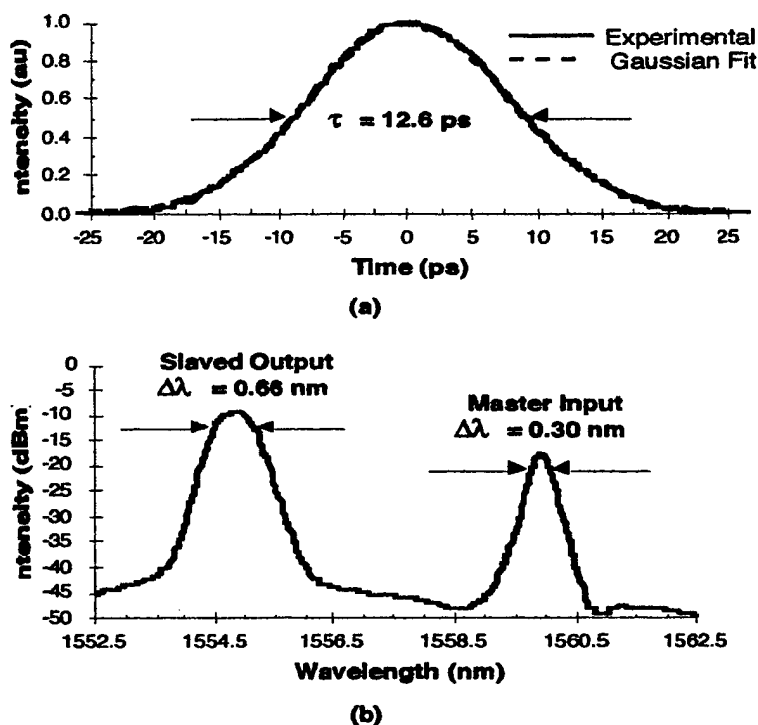


Fig. 13. Output of MQW laser Injection mode locked at its second harmonic

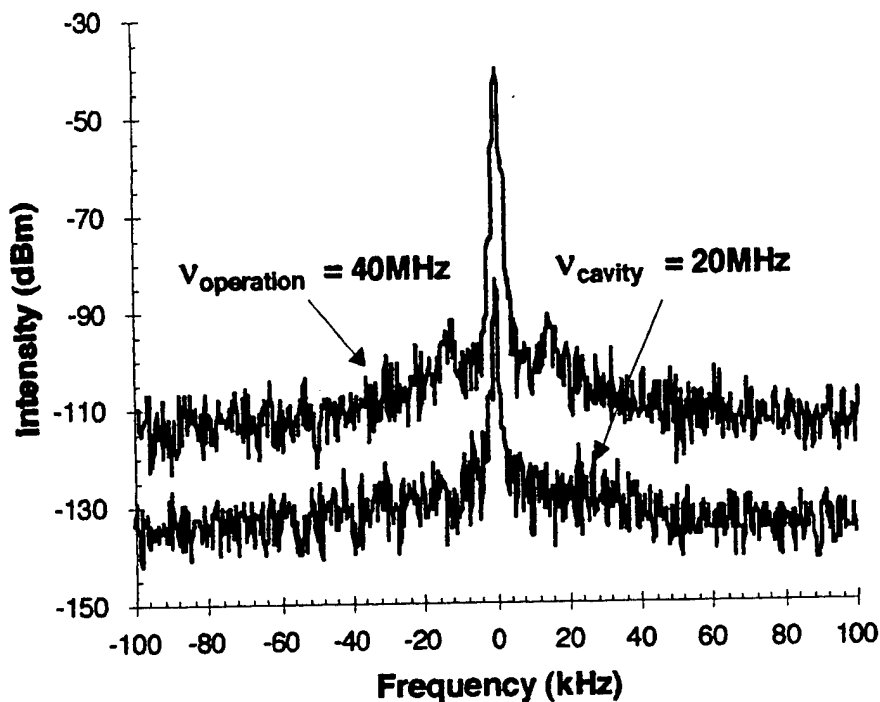


Fig. 14 Power spectrum of the MQW laser operating at its second harmonic

3.2 Summary

We demonstrated that the MQW laser can be injection mode locked at both its fundamental cavity frequency and at the second harmonic of this frequency. The mode locking mechanism is the modulation of the loss in the saturable absorber by the injected pulses. The output of the injection locked laser (pulse duration and spectrum) is the same as when the laser is passively mode locked at its fundamental frequency, the MQW laser is stable over a detuning range of 1.83×10^{-4} fractional bandwidth and is insensitive to the polarization state of the injected signal. At the second harmonic the MQW was not synchronized to the injected signal. Operation at a higher repetition rate was not possible due to a combination of insufficient energy in the cavity and the low intensity of the injected pulses.

3.3 Electrical Mode Locking

The same quantum well structures used to passively mode lock the simple cavity illustrated above can also be used as active mode lockers or fast modulators of the laser output. It has been shown that if an electrical field is applied to a multiple quantum well stack, the absorption of the wells shifts to longer wavelengths due to a quadratic Stark effect. An example of this effect is shown in Fig. 15. In this case the electric field was applied to the quantum wells by embedding them in a pin junction which could be back biased to the voltages indicated in the figure. Here absorptance

is the product of the absorption coefficient a and the thickness l of the well structure. The transmission is then given by $T = e^{-al}$. The absorptance peaks shown at zero applied voltage represent exciton transitions from quantum well ground states to states near the ionization limit. The position of these peaks and hence the value of the saturation flux of the absorber at a given wavelength is determined by the barrier widths. The red shift and broadening of the exciton peaks as a function of applied voltage is shown. Depending on the wavelength, either an increase or decrease of absorptance occurs with applied voltage.

In the laser designs described above the quantum well saturable absorber acts as the second mirror in the laser cavity. If R_1 is the reflectivity of the surface on which the fiber is contacted, T is the transmission of the absorber, and R_2 is the reflectivity of the outside surface, then the effective reflectivity of the structure seen by the cavity is given by:

$$R = R_1 + (1 - R_1)R_2T^2$$

If we assume that the front surface is anti reflection coated so that $R_1 = 0$ and the back surface is coated to give $R_2 = 1.0$, then:

$$R = T^2$$

Thus the effective reflectivity of the quantum well structure is determined by its transmission which can be modulated with an applied voltage. As an example, the effective reflectivity as a function of applied voltage for a wavelength of $1.55 \mu\text{m}$ is given in Fig. 16, using the data presented in Fig 15. The effective reflectivity is reduced by a factor of 2 by the application of 10 volts. At other wavelengths the change in R may, of course, be greater or smaller.

It is clear from the above discussion that the effective reflectivity of the saturable absorber at a fixed wavelength, or the wavelength of maximum reflectivity, can be changed by the application of a voltage to the quantum well structure. If the output of the laser is sensitive to these changes in reflectivity the out put of the laser can be modulated or rapidly tuned by the application of a time varying voltage. In addition, active mode locking at a high harmonic of the cavity might be achieved by the application of a voltage of the appropriate frequency. In fact, a PIN - multiple quantum well device has already been used to initiate mode locking in a fiber laser, but only at the fundamental cavity frequency and with poor pulse shape.

One problem with this idea is found in the fact that, due to their very high gain, the output power of fiber lasers is actually quite insensitive to changes in the reflectivity of the cavity mirrors. One method of enhancing the change in reflectivity produced by a given applied voltage is to incorporate the PIN quantum well device into a Fabry Perot etalon. Changes in the index of refraction produced by the electric field will then lead to much larger changes in the reflectivity of the device. As an example the reflectivity of a Fabry Perot etalon as a function of wavelength is plotted in Fig. 17. Here it is

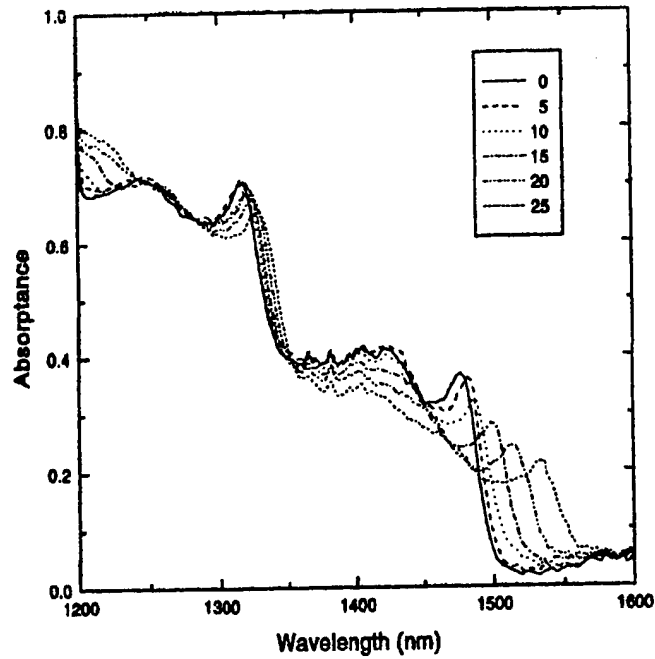


Fig 15. Quantum Well Absorption Spectra as a Function of Applied Voltage
 (From: M. F. Krol, Ph.D. Thesis, Optical Sciences Center, University of Arizona, 1996)

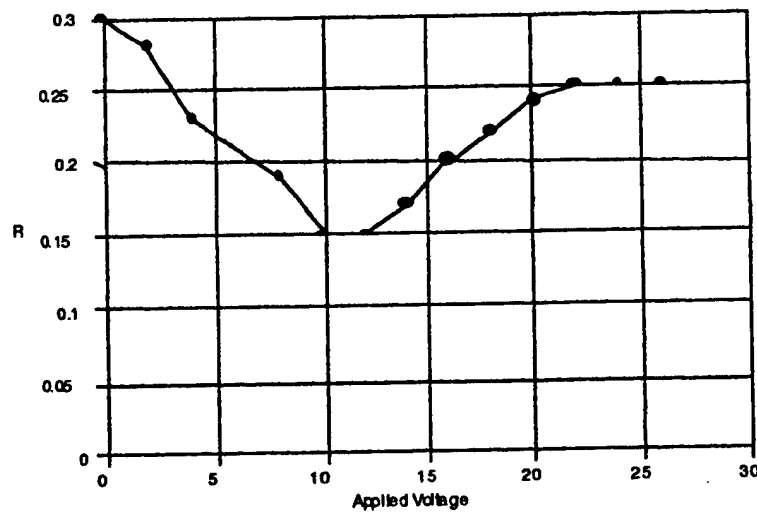


Fig 16. Calculated reflectivity, R, of the saturable absorber as a function of applied voltage.

assumed that the top surface reflectance of the quantum well stack is 0.28 and that the reflectance of the InP substrate is 0.26.

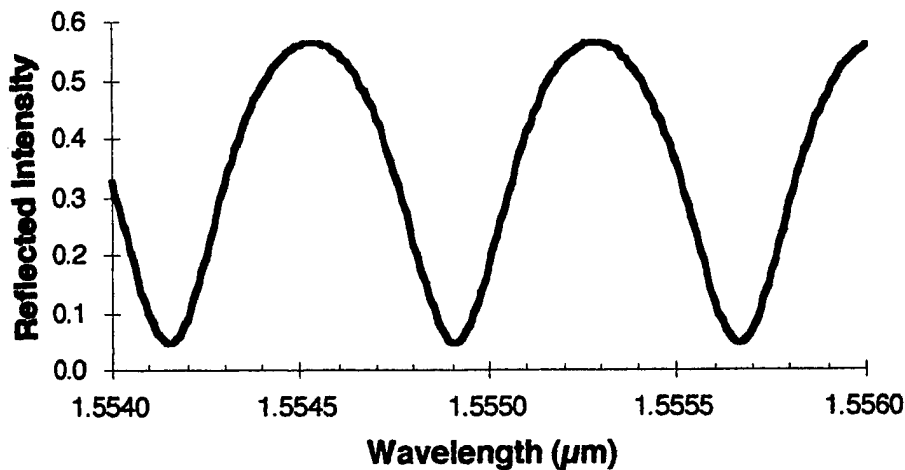


Fig 17. Reflectivity of a saturable absorber in a Fabry Perot etalon.

4.0 References

- [1] I. N. Duling, III and M. L. Dennis, *Compact Sources of Ultrashort Pulses* (Cambridge University, Cambridge, England, 1995).
- [2] I. N. Duling, III, "Subpicosecond all-fiber erbium laser," *Electron. Lett.* **27**, 544 (1991).
- [3] M. E. Fermann, M. J. Andrejco, Y. Silverberg, and M. L. Stock, "Passive modelocking by using nonlinear polarization evolution in polarizing-maintaining erbium-doped fiber," *Opt. Lett.*, **18**, 894 (1993).
- [4] W. H. Loh, D. Atkinson, P. R. Morkel, M. Hopkinson, A. Rivers, A. J. Seeds, and D. N. Payne, "Passively mode-locked Er³⁺ fiber laser using a semiconductor nonlinear mirror," *IEEE Photon. Tech. Lett.*, **5**, 35 (1993).
- [5] B. C. Collings, K. Bergman, S. T. Cundiff, S. Tsuda, J. N. Kutz, J. E. Cunningham, and W. H. Knox, "Short Cavity Erbium/Ytterbium Fiber Lasers Mode-Locked with a Saturable Bragg Reflector," *IEEE J. Select. Topics in Quantum. Electron.*, **3**, 1065 (1997).
- [6] M. J. Hayduk, S. T. Johns, M. F. Krol, C. R. Pollock, and R. P. Leavitt, "Self-starting passively mode-locked tunable femtosecond Cr⁴⁺:YAG laser using a saturable absorber mirror," *Opt. Commun.* **137**, 55 (1997).
- [7] H. A. Haus, "Theory of mode-locking with a fast saturable absorber," *J. Appl. Phys.*, **46**, 3049 (1975).

- [8] H. A. Haus, "Theory of Mode Locking with a Slow Saturable Absorber," *IEEE J. Quantum Electron.*, **11**, 736 (1975).
- [9] F. X. Kärtner, L. R. Brovelli, D. Kopf, M. Kamp, I. Calasso, U. Keller, "Control of solid state laser dynamics by semiconductor devices," *Opt. Eng.*, **34**, 2024 (1995).
- [10] F. X. Kärtner and U. Keller, "Stabilization of solitonlike pulses with a slow saturable absorber," *Opt. Lett.*, **20**, 16 (1995).
- [11] R. P. Davey, N. Langford, A. I. Ferguson, "Interacting solitons in erbium fibre laser," *Electron. Lett.* **27**, 1257 (1991).
- [12] B. C. Barnett, L. Rahman, M. N. Islam, Y. C. Chen, P. Bhattacharya, W. Riha, K. V. Reddy, A. T. Howe, K. A. Stair, H. Iwamura, S. R. Friberg, and T. Mukai, "High-power erbium-doped fiber laser mode locked by a semiconductor saturable absorber," *Opt. Lett.*, **20**, 471 (1995).
- [13] D. von der Linde, "Characterization of the noise in continuously operating mode-locked lasers," *Appl. Phys. B*, **39**, 201 (1986).
- [14] W. I. Kaechele IV, "Mode-locked erbium-doped fiber lasers, synchronization, and noise," Doctoral thesis, Rensselaer Polytechnic Institute, Troy, NY 1997.